Ionic Effects on the Stability and Conformation of Peptide Nucleic Acid Complexes

Sebastian Tomac,[†] Munna Sarkar,[†] Tommi Ratilainen,[‡] Pernilla Wittung,[‡] Peter E. Nielsen,[§] Bengt Nordén,[‡] and Astrid Gräslund*,[†]

Contribution from the Department of Biophysics, Arrhenius Laboratories, Stockholm University, S-10691 Stockholm, Sweden, Department of Physical Chemistry, Chalmers University of Technology, S-41296 Gothenburg, Sweden, and Center for Biomolecular Recognition, The Panum Institute, IMBG, Department of Biochemistry B, Blegdamsvej 3c, DK-2200 Copenhagen N, Denmark

Received February 15, 1996[⊗]

Abstract: Peptide nucleic acid (PNA) is a DNA analogue in which the negatively charged sugar phosphate backbone has been substituted by uncharged *N*-(2-aminoethyl)glycine units. The study of a PNA−DNA duplex and the corresponding DNA−DNA duplex gives a unique opportunity to compare two polyelectrolytes with virtually identical geometry but greatly different linear charge density. The results provide a basis for a study of the applicability of the Poisson−Boltzmann (PB) and counterion condensation (CC) theories. UV and circular dichroism spectroscopy as well as isothermal titration calorimetry (ITC) have been used to study the effect of different ions on the stability and conformation of PNA−DNA, PNA−PNA, and DNA−DNA duplexes having the same base sequences. Cations in general destabilize both antiparallel (N/3′) and parallel (N/5′) PNA−DNA duplexes whereas they stabilize the DNA−DNA duplex. Studies on the effect of monovalent salt such as NaCl on T_m were carried out over a wide range of salt concentrations (0.01 to 5 M). The decrease in the T_m of the N/3′ PNA−DNA duplex with increasing ionic strength in the range of concentrations of 0.01 to 0.5 M, where electrostatic effects predominate, is explained in terms of counterion release upon duplex formation in contrast to the counterion association accompanying the formation of a DNA duplex. The uncharged PNA−PNA duplex shows no significant destabilization in this concentration range. The higher stability of the N/3′ PNA−DNA compared to the DNA−DNA duplex ($\Delta\Delta G \sim -7$ kcal/mol) is ascribed to more favorable entropic contributions consistent with the counterion release that accompanies the PNA−DNA duplex formation. At high salt concentration (>1 M), where electrostatic contributions saturate, similar trends in the decrease in T_m were observed for the three types of duplexes irrespective of their backbone charges. The destabilizing effects of a series of Na salts with various monovalent anions on N/3′ PNA−DNA and PNA−PNA duplexes were found to follow the Hofmeister series, emphasizing the importance of the hydrophobic interaction between nucleobases for the stability of the PNA complexes in high salt concentration.

Introduction

Peptide nucleic acid (PNA) is a new oligonucleotide mimic where the sugar−phosphate backbone has been substituted with *N*-(2-aminoethyl)glycine units to which the nucleobases are attached (Figure 1).[1] Oligonucleotide analogues and mimics like PNA are intensively studied for the purpose of creating new gene-targeting drugs, and also to provide a better understanding of structural features leading to the unique genetic properties of DNA as well as RNA. PNA oligomers containing both purines and pyrimidines bind to complementary single-stranded DNA, RNA, as well as PNA with high affinities,[1,2a,b] whereas homopyrimidine PNA oligomers bind to homopurinic DNA oligomers forming a $(PNA)_2$/DNA triplex.[3,4] Homopyrimidine PNA oligomers have been found to invade double stranded DNA with a concomitant displacement of the DNA

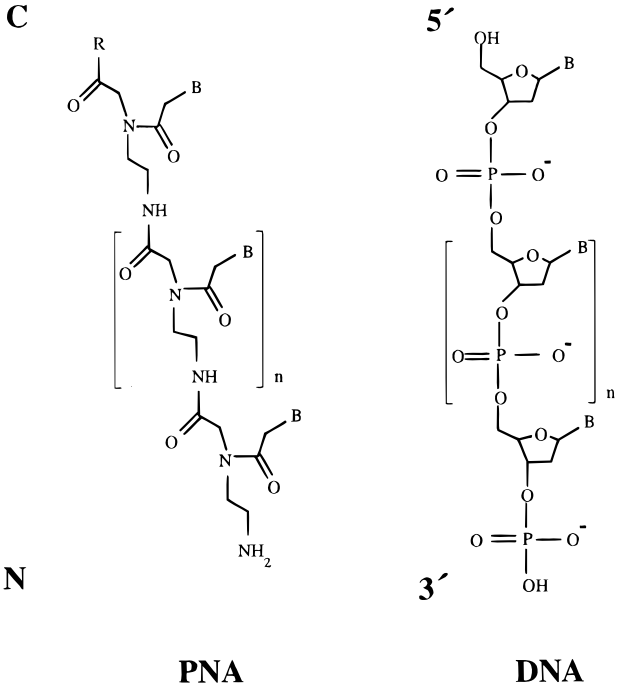

PNA **DNA**

Figure 1. Chemical structure of PNA. B is the nucleobase. The amino terminal is denoted "N", and the carboxy terminal is denoted "C". For comparison the structure of DNA is shown.

* To whom correspondence should be addressed.
† Stockholm University.
‡ Chalmers University of Technology.
§ The Panum Institute.
⊗ Abstract published in *Advance ACS Abstracts,* June 1, 1996.

(1) Nielsen, P. E. *Annu. Rev. Biophys. Biomol. Struct.* **1995**, *24*, 167−183.
(2) (a) Nielsen, P. E.; Egholm, M.; Berg, R. H.; Buchardt, O. *Science* **1991**, *254*, 1497−1500. (b) Egholm, M.; Buchardt, O.; Nielsen, P. E.; Berg, R. H. *J. Am. Chem. Soc.* **1992**, *114*, 1895−1897. (c) Christensen, L.; Fritzpatrick, R.; Gildea, B.; Petersen, K. H.; Hansen, H. F.; Koch, T.; Egholm, M.; Buchardt, O.; Nielsen, P. E.; Coull, J.; Berg, R. H. *J. Pept. Sci.* **1995**, *3*, 175−183.

S0002-7863(96)00495-7 CCC: $12.00

strand that has the same sequence as that of the invading PNA.[1,5] These properties of PNA make them potential candidates for both antisense and antigene drugs. PNA, having a backbone that is structurally homomorphous to the sugar−phosphate backbone of RNA and DNA, has been shown to hybridize with complementary strands of DNA or RNA, following Watson−Crick base pairing rules,[6] either in what has been called a parallel or an antiparallel fashion, i.e. with the N-terminus of PNA located adjacent to the 5′-end or the 3′-end of the oligonucleotide strand, respectively. A PNA strand can also hybridize with another complementary PNA strand to form a helical duplex.[7] PNA forms a B-like helix with DNA[8] and an A-like helix with RNA.[9]

The mixed-sequence PNA duplexes with DNA, RNA, as well as a complementary strand of PNA are found to have enhanced thermal stability compared to the corresponding DNA−DNA or RNA−RNA duplexes, with the highest stability for the PNA−PNA duplex.[1,7] The antiparallel PNA−DNA and PNA−RNA duplexes have been shown to be more stable than the parallel duplexes.[6] It has been found that increasing ionic strength has a destabilizing effect on the PNA−DNA duplexes,[6] but only a few studies report on the effects of ions on the different interactions involving PNA complexes.[5,10−11] It is important to investigate the ionic effects more carefully in order to interpret the behavior of the PNA molecules at physiological conditions, both from a strategical point of view to assess the potentials of PNA for medicinal and biotechnological use and to obtain a better understanding of the basic interactions of PNA as well as DNA in solution. Salts affect the properties of biological macromolecules such as their stability, solubility, and biological activity in widely different manners.[12] At low concentrations (<1 M), salts generally exert their effects on polyelectrolytes through non-specific electrostatic interactions depending on the ionic strength of the medium.[13] By contrast, at high salt concentrations (>1 M), the electrostatic contributions saturate and the salts instead exert specific effects on biopolymers which depend on the nature of the salt and its concentration and also on its indirect effect on the bulk aqueous solvent.[14]

Up to now, studies on ionic effects on biopolymers have been restricted mainly to proteins and nucleic acids and their interactions with various ligands.[13] The synthetic PNA molecule is a unique system in the sense that it represents a combination of some of the aspects of proteins as well as nucleic acids. PNA is expected to have characteristics of its own which are different from those of proteins or nucleic acids. A DNA−DNA duplex with its negatively charged backbone and a PNA−PNA duplex with its neutral backbone represent two extreme situations in terms of electrostatic effects and are expected to respond differently to variations in ionic environments. A PNA−DNA duplex on the other hand represents an intermediate case where only one of the two strands is negatively charged. Systematic studies of the ionic effects on these three types of duplexes could therefore provide information of more general interest and may facilitate the understanding of the complex problem of how salt affects the thermodynamic stability of native biopolymers in different ranges of salt concentrations.

In this study we have investigated the effects of various ions on the thermal stability of the PNA−PNA and PNA−DNA hybrid duplexes and compared these to the effects on a DNA−DNA duplex having the same base sequence as the PNA duplexes, over a wide range of salt concentrations. The results were evaluated using both the counterion condensation (CC) and Poisson−Boltzmann (PB) approaches, which enabled us to compare the applicability of both approaches to describe the polyelectrolyte properties of the complexes. Different cations such as NH_4^+, Na^+ (monovalent), Mn^{2+}, Mg^{2+} (divalent), and spermine (multivalent, $H_2N(CH_2)_3NH(CH_2)_4NH(CH_2)_3NH_2$) as well as monovalent anions such as CH_3COO^-, Cl^-, and ClO_4^- were studied. We have used mainly UV spectrophotometry and isothermal titration calorimetry to investigate the effects of different ions on the thermal stability of PNA−PNA, PNA−DNA, and DNA−DNA duplexes and also to extract the relevant thermodynamic parameters. Circular dichroism spectroscopy was used to elucidate the effects of ions on the backbone conformation of these complexes.

Materials and Methods

PNA Complexes Studied. Parallel, N/5′, and antiparallel, N/3′, PNA−DNA as well as PNA-PNA and DNA−DNA antiparallel duplexes were formed by the following sequences.

The strands used were

PNA1 10-mer	N-GTAGATCACT-C
PNA2 10-mer	N-AGTGATCTAC-C
DNA1 10-mer	5′-GTAGATCACT-3′
DNA2 10-mer	5′-AGTGATCTAC-3′
DNA3 10-mer	5′-CATCTAGTGA-3′
PNA1 15-mer	N-TAGACGTCACAACTA-C
DNA1 15-mer	5′-TAGACGTCACAACTA-3′
DNA2 15-mer	5′-TAGTTGTGACGTCTA-3′

For the PNA sequence "N" represents the free amino group, corresponding to the N-terminal of a peptide, and "C" is the amidated carboxyl terminal, corresponding to the C-terminal of a peptide (Figure 1). The N/3′ or antiparallel orientation is defined as when the 3′ end of the DNA sequence is oriented toward the N-terminal of the PNA and the N/5′ or parallel orientation is defined when the 5′ end of the DNA sequence is oriented toward the N-terminal of the PNA. Antiparallel duplexes (N/3′) were formed between PNA1−DNA2 10-mers, PNA1−DNA2 15-mers, DNA1−DNA2 10-mers, DNA1−DNA2 15-mers, and PNA1−PNA2 10-mers. A N/3′ PNA−DNA 15-mer duplex was also formed using a PNA with an acylated free amino group, thereby removing the single positive charge at the N-terminal. Unless otherwise mentioned, the references in the text are to the 10-mer duplexes.

Sample Preparation for Optical and Circular Dichroism Studies. The 10-mer and 15-mer PNA sequences were synthesized as described previously.[2c] The deoxyribonucleotides were obtained from Symbicom, Umeå, Sweden. They were synthesized according to the phosphotriester method, purified by HPLC, and lyophilized from water. All solutions

(3) (a) Egholm, M.; Nielsen, P. E.; Berg, R. H.; Buchardt, O.; Berg, R. H. *J. Am. Chem. Soc.* **1992**, *114*, 9677−9678. (b) Kim, S. K.; Nielsen, P. E.; Egholm, M.; Buchardt, O.; Berg, R. H.; Nordén, B. *J. Am. Chem. Soc.* **1993**, *114*, 6477−6481.

(4) Betts, L.; Josey, J. A.; Veal, J. M.; Jordan, S. R. *Science* **1995**, *270*, 1838−1841.

(5) (a) Peffer, N. J.; Hanvey, J. C.; Bisi, J. E.; Thomson, S. A.; Hassman, F.; Noble, S. A.; Babiss, L. E. *Proc. Natl. Acad. Sci. U.S.A.* **1993**, *90*, 10648−10652. (b) Nielsen, P. E.; Egholm, M.; Buchardt, O. *J. Mol. Recognit.* **1994**, *7*, 165−170.

(6) Egholm, M.; Buchardt, O.; Christensen, L.; Behrens, C.; Freier, S. M.; Driver, D. A.; Berg, R. H.; Kim, S. K.; Nordén, B.; Nielsen, P. E. *Nature*. **1993**, *365*, 566−568.

(7) Wittung, P.; Nielsen, P. E.; Buchardt, O.; Egholm, M.; Nordén, B. *Nature* **1994**, *368*, 561−563.

(8) Leijon, M.; Gräslund, A.; Nielsen, P. E.; Buchardt, O.; Nordén, B.; Kristensen, S. M.; Eriksson, M. *Biochemistry* **1994**, *33*, 9820−9825.

(9) Brown, S. C.; Thomson, S. A.; Veal, J. M.; Davis, D. G. *Science* **1994**, *265*, 777−780.

(10) Nielsen, P. E.; Egholm, M.; Berg, R. H.; Buchardt, O. *Nucleic Acids Res.* **1993**, *21*, 197−200.

(11) Hanvey, J. C.; Peffer, N. J.; Bisi, J. E.; Thomson, S. A.; Cadilla, R.; Josey, J. A.; Ricca, D. J.; Hassman, F.; Bonham, M. A.; Au, K. G.; Carter, S. T.; Bruckenstein, D. A.; Boyd, A. L.; Noble, S. A.; Babiss, L. E. *Science* **1992**, *258*, 1481−1485.

(12) Von Hippel, P. H.; Schleich T. In *Biological Macromolecules;* Vol. 2, *Structure and Stability of Biological Macromolecules;* Timasheff, S. N., Fasman, G., Eds.; M. Dekker Inc.: New York, 1969; pp 417−574.

(13) Bloomfield, V.; Carpenter, I. L. *Polyelectrolytes; Science and Technology;* Hara, M., Ed.; M. Dekker Inc.: New York, Basel, 1993; pp 77−125.

(14) Collins K. D.; Washabaugh, M. W. *Q. Rev. Biophys.* **1985**, *18*, 323−422.

were prepared with buffers containing 10 mM sodium phosphate (pH 7.0) or 10 mM sodium cacodylate (pH 7.0). $NaClO_4$, CH_3COONa, NaCl, NH_4Cl, $MgCl_2$, $MnCl_2$, or spermine ($H_2N(CH_2)_3NH(CH_2)_4NH(CH_2)_3NH_2$) were obtained from Sigma in pro analysis grade and used without further purification. Equimolar mixtures (1:1 stoichiometry in single strands) of the PNA with the corresponding DNA/PNA sequence were prepared by heating the samples well above their melting temperatures, and then by annealing to form the duplexes. Reproducible melting curves were obtained for each type of duplex. The single-strand absorbance at 25 °C was determined by linear extrapolation of the upper baseline in the UV melting curves. The corresponding 25 °C extinction coefficient was calculated by the nearest neighbor analysis[15,16] assuming that the extinction coefficient of the nucleobases in the PNA is the same as in DNA. The concentration of the oligomers was determined using the extinction coefficient of 1.03×10^5 M^{-1} cm^{-1} for the single-stranded 10-mer and 1.38×10^5 M^{-1} cm^{-1} for the 15-mer studied here. All concentrations are given on a per strand basis unless otherwise mentioned. The hypochromicity observed upon helix formation was determined as[15]

$$\text{hypochromicity} = (A_S - A_D)/A_S \tag{1}$$

where A_D and A_S are the double-strand and single-strand absorbance at temperatures as close as possible to the beginning and end of the helix-to-coil transition, respectively.

UV Spectroscopy. Absorbance versus temperature profiles were obtained at 260 nm with a Cary 3E or 4 spectrophotometer interfaced with a NEC computer. Quartz cells with path lengths of 10 and 2 mm were used to allow measurements over the range of oligomer concentrations used. The temperature of the sample was increased continuously at a rate of 0.5 °C per min using an ethylene glycol water circulating bath (Lauda RM6) fitted with a thermoregulator (Eurotherm 808).

Thermodynamic Analysis of the Melting Data. The UV melting curves were analyzed to obtain van't Hoff transition enthalpies. This analysis requires converting the experimental absorbance vs temperature curve into a melted fraction vs temperature curve. The melted fraction in single strands (f) vs temperature (T) plots were obtained by fitting the melting profile to a two-state transition model, with linearly sloping lower and upper baselines.[16] The T_m's were obtained directly from the temperature at $f = 0.5$. A correction was done to take into account the difference between the bath and sample temperature. From repeated measurements we estimated approximate uncertainities in the estimated T_m values. We found ranges of ±0.5 °C for the lower salt concentrations (<0.5 M) and rising to ±2 °C at the highest (5 M) salt concentration. The thermodynamic parameters were determined from the melting curves using two methods.

(a) From van't Hoff's Plot or the ln *K* vs 1/*T* Plot. Values of K, the equilibrium constant, were determined at each temperature using the equation[15,16]

$$K = (1 - f)/[(C_T/n)^{n-1} f^n] \tag{2}$$

where C_T is the total strand concentration and n is the molecularity of the reaction. Only points with $0.15 < f < 0.85$ were used in the van't Hoff's plot since this is a region where the K values are most precise. For a two-state transition, if ΔH is independent of the temperature, then a plot of ln K vs $1/T$ is linear with $(-\Delta H/R)$ as the slope and $(\Delta S/R)$ as the intercept. The slopes and the intercept of the van't Hoff's plot were obtained by linear regression analysis with a correlation coefficient ~0.98.

(b) From the Plot of $1/T_m$ vs ln (concentration). The ΔH values were also obtained from the slope of the $1/T_m$ (K^{-1}) vs ln C_T (concentration) plot which should be a linear function, using the relation[16]

$$\text{slope} = (n - 1)R/\Delta H \tag{3}$$

where n is the molecularity of the association reaction and R is the gas constant. This relation is true for both self-complementary and non-self-complementary sequences. ΔS is determined from the intercept at ln $C_T = 0$, where for a self-complementary molecule the following relation applies[16]

$$\text{intercept} = [\Delta S - (n - 1)R \ln 2 + R \ln n]/\Delta H \tag{4}$$

and for a non-self-complementary molecule

$$\text{intercept} = [\Delta S - (n - 1)R \ln 2n]/\Delta H \tag{5}$$

Isothermal Titration Calorimetry (ITC). A MicroCal ITC MC-2 system was used in conjuction with an electronically controlled circulating water bath. All samples used in the ITC experiments were performed in 10 mM sodium phosphate buffer, pH 7.7. The temperature was held constant at 25 °C for all experiments. A solution of one of the strands (6 μM of PNA2 or DNA2, respectively) was placed in the cell (volume 1.36 mL) and the titrant solution (0.138 mM PNA1) in the 100-μL syringe, whose needle is designed as a paddle-shaped stirrer rotating at 400 rpm. The plunger is controlled by a stepping motor, allowing precise injections smaller than 1 μL. Typically 20 injections of 4 μL each and 5 min apart were made. The integrated peaks (pulses) of the heat production of each injection were calculated, the first 5−10 directly giving the enthalpy of interaction (ΔH). The calorimetric enthalpy of interaction was corrected for the self-melting of PNA (see text).

Theoretical Models for the Effects of Salts on the Thermal Stability of Polynucleotides. The counterion condensation (CC) theory for polyelectrolytes[13,17−22] and the cylindrical cell Poisson−Boltzmann (PB) model[23−25] have been used to describe the stabilizing effect of increasing monovalent cation concentration on DNA duplexes. DNA in a double-helical form has a higher charge density as compared to the single-stranded form. Helix formation is accompanied by an increase in counterion association. An increase in bulk salt concentration stabilizes the state with higher charge density as compared to the coiled state, resulting in an increase in T_m of the helix-to-coil transition. The differential number of counterions between duplex and single-stranded states, for DNA−DNA duplexes, remains constant over a salt concentration of ~10^{-1} to 10^{-3} M.[17,22] At low to moderate monovalent (M^+X^- salt concentrations (10^{-3} to 10^{-1} M) the transition temperature, T_m, of a polynucleotide double helix is function of the logarithm of the mean activity $a_\pm$ (or concentration $[M^+]$) of the salt (e.g. NaCl).[21,26] The value of $dT_m/d \log[Na^+]$ is a characteristic property of the polynucleotide system and has been related to the thermodynamic differential counterion association parameter per phosphate group ($\Delta\psi$), through[21]

$$dT_m/d \log[Na^+] = 0.9(2.303RT_m^2/\Delta H)(N_u \Delta\psi) \tag{6}$$

where ΔH is the helix (h)-to-coil (c) transition enthalpy, R is the gas constant, expressed in [cal/(mol K)], and N_u is the number of phosphates per cooperative melting unit. For a two-state melting transition in oligonucleotide duplexes this cooperative unit is equal to the entire duplex. The 0.9 correction factor corresponds to the conversion of mean ionic activities to concentration, and 2.303 is the conversion from $\log_e$ to $\log_{10}$ units. The ratio $RT_m^2/\Delta H$ has been found experimentally to be constant (within ±10% experimental error range)[21] for DNA within the small range of salt concentrations over which eq 6 is valid.

(15) Puglisi, J. D.; Tinoco, I., Jr. *Methods Enzymol.* **1989**, *180*, 304−325.
(16) Marky, L. A.; Breslauer, K. J. *Biopolymers* **1987**, *26*, 1601−1620.
(17) Manning, G. S. *J. Chem. Phys.* **1969**, *51*, 924−933.
(18) Manning, G. S. *Biopolymers* **1972**, *11*, 937−949.
(19) Manning, G. S. *Q. Rev. Biophys.* **1978**, *11*, 179−246.
(20) Record, M. T., Jr. *Biopolymers* **1975**, *14*, 2137−2158.
(21) Record, M. T., Jr.; Anderson, C. F.; Lohman, T. M. *Q. Rev. Biophys.* **1978**, *11*, 103−178.
(22) Anderson, C. F.; Record, M. T., Jr.; Hart, P. A. *Biophys. Chem.* **1978**, *7*, 301−316.
(23) Bond, J. P.; Anderson, C. F.; Record, M. T. *Biophys. J.* **1994**, *67*, 825−836.
(24) Anderson, C. F.; Record, M. T. *Structure and Dynamics;* Clementi, E., Sarma, R., Eds.; Adenine Press: New York, 1983; pp 301−319.
(25) Frank-Kamenetskii, M. D.; Anshelevich, V. V.; Lukashin, A. V. *Sov. Phys. Usp.* **1987,** *30*, 317−330.
(26) Krakauer, H.; Sturtevant, J. M. *Biopolymers* **1968**, *6*, 491−512.

In order to interpret the data in terms of polyelectrolyte properties of the complexes, further theoretical modeling is required, using the CC theory and the PB model. The CC theory treats a polynucleotide as an infinite linear array of univalent charges with average axial spacing "*b*". The extent of association of monovalent counterions with this polyion is given by the dimensionless structural parameter "ξ" defined as[19]

$$\xi = e^2/\epsilon kTb = b_j/b \tag{7}$$

where e is the electronic charge, ϵ is the bulk dielectric constant of the solvent, k is the Boltzmann's constant, and T is the temperature in Kelvin; b_j is the Bjerrum length, or the distance at which the Coulomb energy between two unit charges equals the thermal energy. For water at 25 °C $b_j = 7.14$ Å. ξ is related to the thermodynamic differential counterion binding per phosphate, $\Delta\psi$, through the relation.[19,21]

$$\Delta\psi = {}^1/_2(\xi_c^{-1} - \xi_h^{-1}) \tag{8}$$

where ξ_c^{-1} is used for single-stranded (coil) DNA and ξ_h^{-1} is used for the DNA in the duplex form.[19,21]

As a more elaborate alternative to the CC theory, PB theory has been used to describe the thermodynamic differential counterion association parameter ($\Delta\psi$) in terms of the stoichiometrically-weighted difference in the preferential interaction parameter ($\Delta\Gamma$),[23,24]

$$\Delta\psi = -2\Delta\Gamma \tag{9}$$

Here $\Delta\Gamma = \Gamma_c - \Gamma_h$, i.e., the difference in the coil and helix states. At sufficiently high dilution of a cylindrical polyelectrolyte and in sufficient excess of salt, the following relation applies:[23]

$$\Gamma = -[2\xi - \xi^2 + S_a]/4\xi \tag{10}$$

ξ is defined as previously, and S_a is proportional to the local concentration of electrolyte ions on the polyion surface:[24]

$$S_a = 2\xi V[C_+(a) + C_-(a)] \tag{11}$$

where $V = N_A\pi a^2 b$ is the volume per polyion monomer excluded at contact between a small ion (modeled as a hard sphere) and the polyion (modeled as a hard cylinder), N_A is Avogadro's number, $C(a)$ denotes the local concentration of univalent cations and anions at the polyion surface ($r = a$), and "*b*" is the length of the polyion unit or average axial charge spacing.

$C_+(a)$ and $C_-(a)$ can be evaluated from the Boltzmann expression: $C(r) = C(\mathrm{R})\exp(-z\phi(r))$. $C(\mathrm{R})$ is the bulk ion concentration and z is the valence of the ion. $\phi(r)$ is the mean electrostatic potential expressed in units of e/kT. The potential is obtained by numerically solving the Poisson−Boltzmann equation for a uniform and continuously charged cylindrical polyion:[23,24]

$$1/r[\delta(r\phi'(r))/\delta r] = (4\pi N_A e^2)/(\epsilon kT)[C_+(\mathrm{R})e^{\phi(r)} - C_-(\mathrm{R})e^{-\phi(r)}] \tag{12}$$

with the following boundary conditions: $\phi(r) = 0$ at infinite distance from the cylinder, and $\delta\phi(r)/\delta r = -2\xi/a$ at $r = a$. For solving the Poisson−Boltzmann equation a modified version of part of the Monte Carlo self consistent field simulation program SFMK was used.[27,28] The calculated values of $\Delta\Gamma$ at different ionic strengths were fitted to a fourth order polynomial function of log[Na^+]. The polynomial was fitted by nonlinear least-squares fitting to the calculated points, and a fourth order polynomial was arbitrarily chosen because it gave a better fit than a quadratic polynomial (a quadratic polynomial was used in ref 23). The polynomial function was multiplied with the appropriate constants from eqs 9 and 6. The function was then integrated, and appropriate integration constants were selected so that the calculated curves of T_m vs log[Na^+] would coincide on one observed T_m point[23] (Figure 4b).

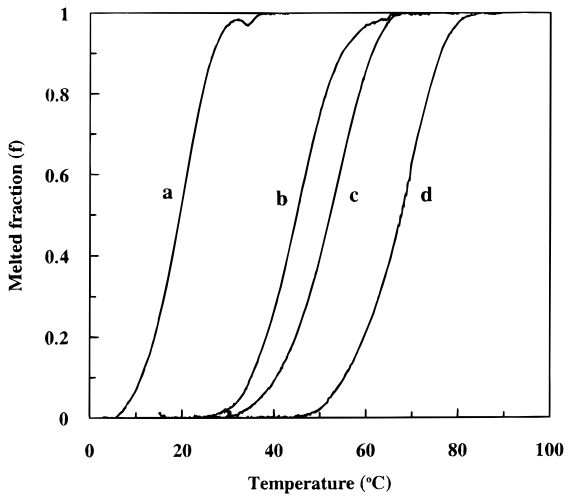

Figure 2. Typical melted fraction (f) vs temperature curves corrected for baseline slopes (as described in the text) for DNA−DNA (a), N/5′ PNA−DNA (b), N/3′ PNA−DNA (c), and PNA−PNA (d). Prior to the melting each hybridization was achieved by mixing equimolar amounts of the complementary single strands and then heating above the respective T_m, followed by slow cooling. The melting curves were recorded in 10 mM sodium phosphate buffer at pH 7.0, without any added salt. The strand concentrations range from 6 to 8.5 μM.

Circular Dichroism Spectroscopy. CD spectra were recorded on a Jasco model 720 spectropolarimeter equipped with a thermoelectrically controlled cell holder, using the same samples that were used for the UV melting studies. Each spectrum reported here is an average of at least four scans and recorded with 1 cm path length cuvettes.

Results

UV Absorbance Melting Curves. The helix-to-coil transitions of antiparallel (N/3′) and parallel (N/5′) PNA−DNA and PNA−PNA duplexes and the corresponding DNA−DNA were characterized by UV melting curves monitored by the absorbance value at 260 nm. All complexes showed a broad monophasic melting transition characteristic of oligonucleotides. Hypochromicities of 14−16% were observed for the formation of 10-mer N/3′ and N/5′ PNA−DNA duplexes as well as the corresponding DNA−DNA duplex and approximately 22% for the 10-mer PNA-PNA duplex. Increasing the NaCl concentration from 0 to 1 M did not affect the hypochromicities of DNA−DNA and N/3′ PNA−DNA duplexes significantly (±3%), but for the PNA−PNA duplex the hypochromicity decreased from 22% to 13% from 0 to 1 M NaCl. This suggests that the PNA−DNA duplexes have similar stacking as the DNA−DNA duplex and that it remains unaffected at moderate salt concentration (≤1 M), whereas the stacking is significantly different in the case of a PNA−PNA duplex with the same base sequence as the other two duplexes. The decrease in hypochromicity with increasing salt concentration could reflect decreased base stacking interactions.

Typical melted fraction (f) vs temperature (T) curves are shown in Figure 2 for the 10-mer complexes in 10 mM sodium phosphate buffer (pH 7.0) with no added salt. At this low ionic strength both the antiparallel and parallel PNA−DNA duplexes have higher thermal stability (T_m = 52.1 °C for N/3′ and 44.9 °C for N/5′, curves b and c in Figure 2) than the DNA−DNA duplex (19.5 °C, curve a in Figure 2). The PNA−PNA duplex has the highest stability with a T_m of 66.1 °C (curve d in Figure

(27) Vorontstov-Velyaminov, P. N.; Lyubartsev, A. P. *Mol. Simul.* **1992**, *9*, 285−306.
(28) Vorontstov-Velyaminov, P. N.; Lyubartsev, A. P. *J. Biomol. Struct. Dyn.* **1989**, *7*, 739−747.
(29) Record, M. T., Jr. *Biopolymers* **1967**, *5*, 975−992.

Table 1. Melting Temperature (T_m, °C) of PNA−DNA Duplexes at Different Salt/Polyamine Concentrations

	NaCl concn (M)[a]		
	0.0	0.05	0.5
DNA−DNA	19.5	31.0	43.0
N/3′ PNA−DNA	52.1	51.0	44.7
N/5′ PNA−DNA	44.9	41.5	34.7
PNA−PNA	66.1	65.4	64.3
	$MgCl_2$ concn (M)[b]		
	0.0	0.005	0.05
DNA−DNA	16.5	38.7	45.7
N/3′ PNA−DNA	54.1	51.7	48.3
N/5′ PNA−DNA	46.4	41.6	38.8
PNA−PNA	66.7	66.4	65.8
	spermine concn (μM)[a]		
	0.0	10.0	100.0
DNA−DNA	19.5	25.8	38.8
N/3′ PNA−DNA	52.1	47.5	45.7
N/5′ PNA−DNA	44.9	42.6	40.8
PNA−PNA	66.1	64.8	63.5

[a] Buffer: 10 mM sodium phosphate (pH 7.0). [b] Buffer: 10 mM sodium cacodylate (pH 7.0)

2). Unlike single-stranded DNA, single-stranded PNA's also showed two-state-like melting transitions similar to the helix-to-coil transition in DNA. The melting transition of the single-stranded PNA's is somewhat concentration dependent (data not shown). The detailed behavior of single-stranded PNA and its sequence dependence will be the subject of a separate study and is not further discussed here.

Effects of Different Cations on the Thermal Stability of the Duplexes. Table 1 shows the effect of increasing concentrations of monovalent (NaCl), divalent ($MgCl_2$), and multivalent (spermine) cations on the stability of the 10-mer duplexes as reflected in the T_m values. Increasing concentration of cations resulted in stabilization of DNA−DNA duplexes whereas the PNA−DNA duplexes (both N/3′ and N/5′) were destabilized. The T_m of PNA−PNA did not show significant changes over the different salt ranges as shown in Table 1. For the N/3′ and N/5′ PNA−DNA hybrids the destabilizing effects increased with the valence of the cation. Mn^{2+} and NH_4^+ gave similar destabilizing effects as did Mg^{2+} and Na^+ (data not shown). A significant lowering of the T_m for the N/3′ and N/5′ PNA−DNA duplexes was observed with spermine even at low concentrations ranging from 0 to 100 μM (Table 1).

At higher concentrations of spermine (>1 mM) the PNA−DNA and the corresponding DNA−DNA duplex precipitated whereas the PNA−PNA duplex remained in solution. For the DNA−DNA duplex the precipitation was more pronounced, resulting in a larger decrease in optical density than for the corresponding PNA−DNA solution. This indicates that the effect of polyvalent cations like spermine may primarily be on the DNA strand. The hypochromicity observed in the DNA−DNA and the N/3′ PNA−DNA melting experiments remained largely unaffected by the addition of ions whereas in the case of N/5′ PNA−DNA the hypochromicity decreased substantially.

Thermodynamic Profiles for Duplex Formation. Thermodynamic parameters for the duplex formation were determined in 10 mM sodium phosphate buffer at pH 7.0 (Table 2) from the melting curves, either from the slope and intercept of a $1/T_m$ vs C_T plot or using van't Hoff's plots (see Materials and Methods). Thermodynamic parameters calculated by the two methods were found to be in good agreement (±10%), which indicates that baselines were properly subtracted. Linear van't Hoff's plots were obtained in all cases. In addition, isothermal titration calorimetry (ICT) was used to determine ΔH for duplex formation of N/3′ PNA−DNA and PNA−PNA complexes at 25 °C. These values were found to be −35 kcal/mol for N/3′ PNA−DNA and −26 kcal/mol for PNA−PNA. It should be noted that these ΔH values are the sum of the parameters for formation of the duplexes and breaking of any self structure formed by single-stranded PNA. The thermodynamical parameters determined from the melting curves (ΔH = −63 and −78 kcal/mol, respectively) involve only the formation of the duplexes. Table 2 includes the parameters evaluated for single-strand PNA "melting" from studies of PNA alone at the same concentration as PNA in the duplexes. If the stochiometrically weighted contribution from the breaking of the single-stranded PNA self structure is taken into consideration (Table 2), the ΔH determined by titration calorimetry and the thermodynamic parameters determined by van't Hoff's plots are in reasonably good agreement for both types of duplexes. This agreement indicates that the assumptions (two-state model and temperature-independent ΔH) made for the evaluation of the thermodynamic parameters should be reasonably correct.

Table 2. Thermodynamic Parameters for the Formation of PNA 10-Mer Complexes in 10 mM Sodium Phosphate without Added Salt[a]

sample[b]	ΔH_{vH} (kcal/mol)	$T\Delta S_{vH}$(298K) (kcal/mol)	ΔG_{vH}(298K) (kcal/mol)	T_m (°C)
DNA−DNA	−68	−62	−6	19.5
N/3′ PNA−DNA	−63	−50	−13	52.1
PNA−PNA	−78	−60	−18	66.1
PNA 1	−60	−48	−12	42.4
PNA 2	−66	−53	−13	45.8

[a] From Van't Hoff's plots for the formation of the duplexes for DNA−DNA, N/3′ PNA−DNA, PNA−PNA and for the formation of single-stranded PNA self-structure. The values given in parantheses are the maximum uncertainities of ΔH (±5%); ΔS (±5%); ΔG (±5%); T_m(±0.5 °C). [b] The concentrations in single strands were approximately 5 μM for the duplexes and 2.5 μM for the single-stranded PNA 1 and 2.

Within the experimental error range the ΔH values are not significantly different for the 10-mer N/3′ PNA−DNA and DNA−DNA, indicating a similar type of duplex structure in both cases. However, ΔS for the N/3′ PNA−DNA is less negative (i.e. less unfavorable) than for the corresponding DNA−DNA (Table 2). The higher stability (free energy ΔG ~ 7 kcal/mol more favorable), observed in the case of N/3′ PNA−DNA as compared to that of DNA−DNA, is therefore ascribed to more favorable entropic contributions reflecting a counterion release upon duplex formation, as will be discussed in the following sections. By contrast, the higher stability of the PNA−PNA complex (ΔG ~ 12 kcal/mol more favorable) is due to a favorable enthalpic contribution to the free energy (Table 2).

Effect of Monovalent Salt on the Stability of the Duplexes. To further study the observed destabilizing effect of ions on PNA−DNA duplex and salt effects in general on the thermodynamic stability of PNA−PNA, as compared to that of DNA−DNA, we chose the simplest case of the effect of a M^+X^- salt such as NaCl over a wide range of salt concentrations (0 to 5 M). Figure 3a shows the effect of increasing NaCl concentration on T_m for 10-mer PNA−PNA, N/3′ PNA−DNA and DNA−DNA duplexes. At low to moderate salt concentration (≤0.5 M) the T_m of the DNA−DNA increases with NaCl concentration and then levels off around 1 M NaCl. This is consistent with previous observations.[20,26,29] In contrast, increasing the NaCl concentration in the 0 to 1 M range resulted in a continuous decrease in the T_m values of N/3′ PNA−DNA such that around

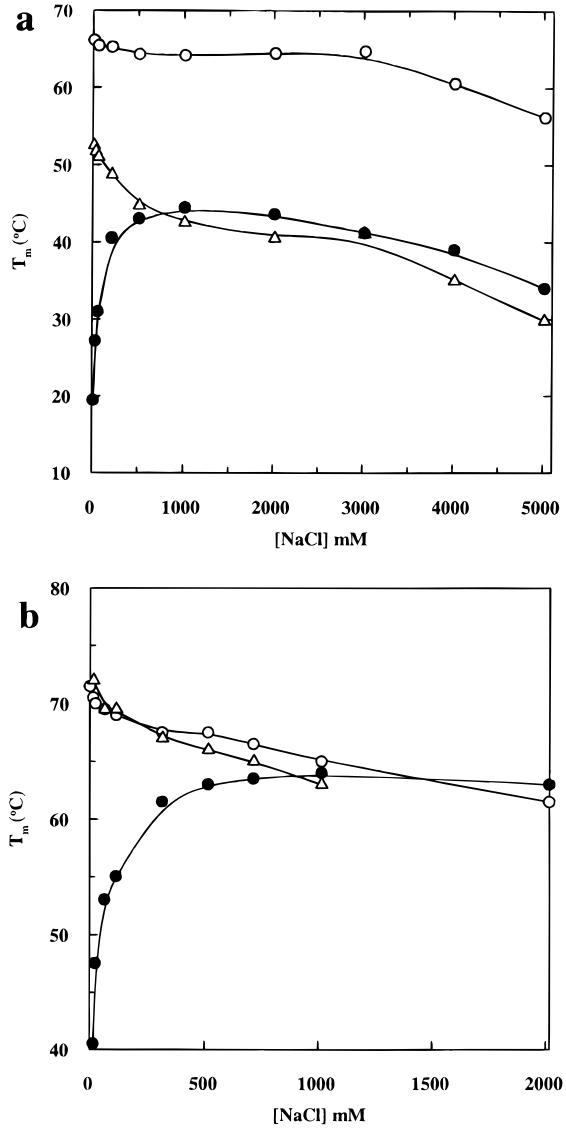

Figure 3. Effects of ionic strength (0−5 M NaCl in 10 mM sodium phosphate, pH 7.0) on the T_m of PNA complexes compared to the corresponding DNA−DNA duplex: (a) PNA−PNA (○), N/3′ PNA−DNA (△), and DNA−DNA (●) 10-mer duplexes; (b) N/3′ PNA−DNA (△), N(ac)/3′ PNA−DNA (the PNA strand has an acylated N-terminal (○)), and DNA−DNA (●) 15-mer duplexes.

1 M of NaCl there was no significant difference in the thermal stability of N/3′ PNA−DNA and DNA−DNA as reflected in their similar T_m values (Figure 3a). The PNA−PNA duplex showed no significant destabilization with NaCl concentration within the same salt range. The difference in behavior of N/3′ PNA−DNA with that of PNA−PNA at NaCl concentrations below 1 M could therefore be attributed to the presence of a negatively charged single strand in the case of N/3′ PNA−DNA, which makes it behave like a polyelectrolyte. At high concentration (>1 M) of NaCl, all the complexes studied were destabilized as reflected in a decrease in the T_m values (Figure 3a).

A similar dependence of T_m on NaCl over the entire range of salt concentrations studied was observed also for 15-mer duplexes (Figure 3b), indicating that this behavior is independent of the chain length. In addition another N/3′ PNA−DNA duplex was studied, where the PNA strand had an acylated amino terminal that removed the single positive charge on the PNA strand. No significant difference in the dependence of T_m on NaCl concentration was seen when comparing the acylated and non-acylated 15-mer N/3′ PNA−DNA (Figure 3b).

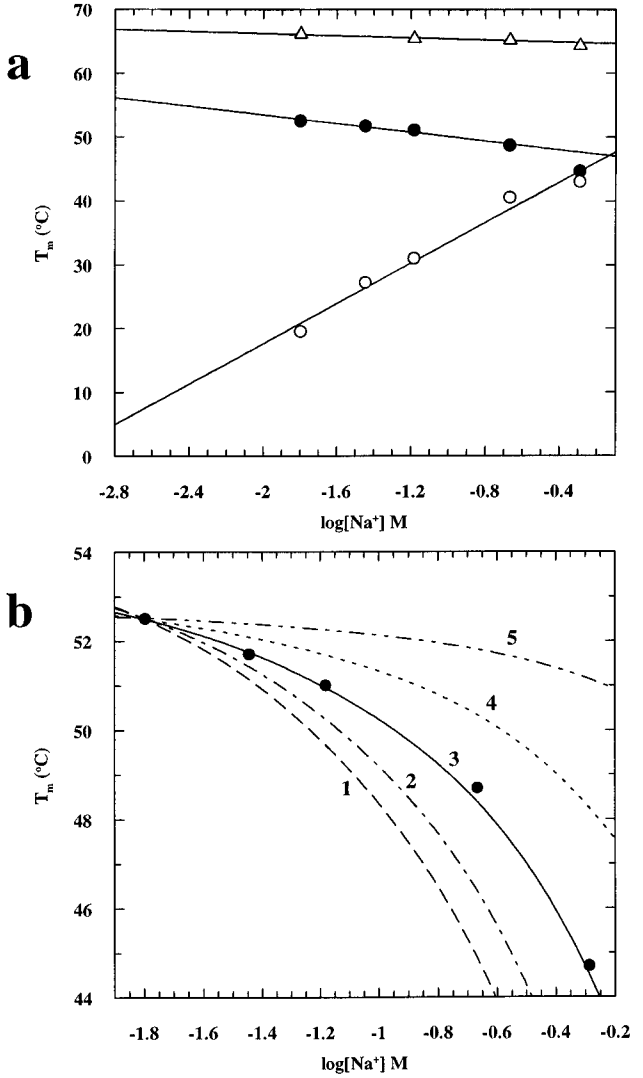

Figure 4. (a) Salt dependence up to 0.5 M NaCl of the T_m for the 10-mer duplexes in 10 mM sodium phosphate, pH 7.0: PNA−PNA (△), N/3′ PNA−DNA (●), and DNA−DNA (○). For the linear fitting only points below 0.5 M of Na^+ were used. The straight lines were fitted to the experimental points by linear regression. (b) Experimental points of T_m vs log[Na^+] for N/3′ PNA−DNA for NaCl in the concentration range 0−0.5 M. The theoretical curves were obtained from nonlinear Poisson−Boltzmann theory as described. Cylinder dimensions used were $b_c = 3.4$ Å, $b_h = 3.4$ Å, $a_c = 6.9$ Å, and $a_h =$ 10 (curve 1), 9.4 (curve 2), 8.6 (curve 3), 7.8 (curve 4), and 7.2 Å (curve 5). The curves were normalized to coincide with the experimental T_m at log[Na^+] = −1.8.

Counterion Association or Release at Low-to-Moderate NaCl Concentration. Unlike the PNA−PNA duplex with its uncharged backbone, both the N/3′ PNA−DNA and the DNA−DNA oligonucleotide duplexes are polyelectrolytes. At low to moderate Na^+ concentrations (10−500 mM) the plots of transition temperature T_m vs log[Na^+] follow a linear relationship in the case of both 10-mer DNA−DNA and N/3′ PNA−DNA (Figure 4a). A linear regression analysis of the plot of T_m vs log[Na^+] (Figure 4a) allowed us to estimate the slopes (dT_m/d log[Na^+]), which are proportional to the thermodynamic differential number of bound/released counterions between the single-stranded and duplex state ($\Delta\psi$ per phosphate) given by eq 6. The evaluated values of the slope are 15.9 K for the 10-mer DNA−DNA and −3.4 K for the N/3′ PNA−DNA 10-mer duplexes. The positive slope obtained for DNA−DNA is characteristic of the counterion association process that takes place upon DNA helix formation.[19−21] By similar reasoning

Table 3. The Thermodynamic Differential Counterion Association Parameter[a] ($\Delta\psi$) and the Parameters Used To Calculate It

10-mer sample	$dT_m/d[Na^+]$ (K)	$RT_m^2/\Delta H$ (K)	$\Delta\psi^b$ [mol (mol of duplex)$^{-1}$]
DNA−DNA	15.9	2.74	0.15
N/3′ PNA−DNA	−3.4	3.52	−0.05

[a] Values are taken in 10 mM sodium phosphate buffer at pH 7.0, and were adjusted to the desired ionic strength with NaCl. The slopes of the T_m vs log Na^+ plots were obtained by least-squares analysis with regression coefficients of at least ±98%. The values of $RT_m^2/\Delta H$ represent the average of at least three observations in the range of 10−100 mM Na^+, with an absolute error of ±8%. The error ranges of $\Delta\psi$ are ±10%. [b] The tabulated $\Delta\psi$ was used for CC calculations only.

the negative slope obtained for N/3′ PNA−DNA (Figure 4a) may be attributed to a counterion release upon helix formation rather than counterion uptake as in the case of DNA−DNA. It should be noted that the T_m of PNA−PNA duplex shows little or practically no dependence on log[Na^+] in this range of salt concentrations (Figure 4a) with a slope of −0.8. From the straight lines of Figure 4a and eq 6 with known values of ΔH (Table 2) we were able to evaluate values of the thermodynamic differential counterion association parameter, $\Delta\psi$, for N/3′ PNA−DNA as well as DNA−DNA duplexes (Table 3). For the N/3′ PNA−DNA, $\Delta\psi$ is −0.05, the negative value indicating counterion release upon duplex formation.

Two theories have been used to describe the ionic effects on the melting temperature of DNA duplexes, the counterion condensation (CC) theory[17−19,21] and the cylindrical cell Poisson−Boltzmann (PB) model.[23,25] In these models the helical structure is simplified to a linear array of charges (CC) or to a cylinder (PB).

In the CC theory only the difference in axial charge spacing determines the magnitude of $\Delta\psi$. Equation 8 can be rewritten as:

$$\Delta\psi = {}^1/_2 b_j(b_c - b_h) \tag{13}$$

The axial charge spacing b_h for the B form DNA duplex is 1.7 Å, which is merely the familiar 3.4 Å base plane distance of the B form divided by the two phosphate groups per base pair. Using this value for b_h and the $\Delta\psi$ value for the 10-mer DNA−DNA duplex ($\Delta\psi$ = 0.15 from Table 3) we can determine b_c from eq 13 as 3.7 Å. This is consistent with the value for the coil form of polymeric DNA ($b_c = 3.9 \pm 0.3$ Å).[30] Since the melting of 10-mer N/3′ PNA−DNA duplex will give the same DNA coil form as the melting of 10-mer DNA−DNA duplex, we used b_c= 3.7 Å and the $\Delta\psi$ value from Table 3 for N/3′ PNA−DNA duplex to calculate b_h from eq 13. This gave the calculated value of b_h = 4.4 Å which is considerably larger than the 3.4 Å base plane distance of the B form DNA helix.

A more rigorous approach to the calculations of electrostatic potentials of linear polyelectrolytes like DNA is based on the solution of the nonlinear Poisson−Boltzmann equation (NLPB).[13,31,32] The NLPB approach has been used to describe the salt effects on the helix−coil transitions of DNA,[23,25] based on a cylindrical model of DNA with uniform charge density. In the previous studies the DNA helix was approximated with a cylinder with axial charge spacing (b_h) of 1.7 Å and cylinder radius (a_h) of ∼9.4 Å.[23] The coil axial charge spacing (b_c) was estimated as ∼3.4 Å,[23] being independent of the helical radius (a_h). The coil radius (a_c) was estimated as 6.9 Å.[23] Using the cylindrical PB model we found that the structure parameters b_h = 1.7 Å, a_h = 9.4 Å, b_c = 3.4, and a_c = 6.9 Å gave a reasonable approximation for our DNA−DNA melting data (data not shown). To model the T_m dependence on ionic strength for the N/3′ PNA−DNA helix we used a cylindrical model and the same structural features for the coil DNA cylinder as used to describe the DNA−DNA melting. For the N/3′ PNA−DNA helix we assumed half the axial charge density, i.e. b_h = 3.4 Å, as compared to the DNA−DNA helix. Choosing varying values of the duplex radius a_h in the interval 7.2 to 10.0 Å, curves of T_m as a function of log[Na^+] could be calculated based on eqs 9−13. We found that a_h = 8.6 Å gave a good fit to the observed data (Figure 4b).

Effect of High Salt Concentration on the Thermal Stability of the Duplexes. At high concentrations of NaCl (>1 M) all the complexes studied were destabilized as shown in Figure 3a. Above a NaCl concentration of 2 M the decrease in T_m for the three types of duplexes follows a very similar trend suggesting that the predominant effect responsible for the destabilization is the same for the duplexes, irrespective of the presence or lack of charges on the backbone. At high salt concentration (>1 M) the electrostatic interactions saturate and various neutral salts exert their specific effects on stabilizing or destabilizing protein structure predominantly through their indirect effect on the surrounding aqueous solvent.[12,14] The effectiveness in decreasing the solubility in water of nonpolar molecules or affecting the stability of specific conformation of proteins or nucleic acids (as reflected in the T_m values) depends on the nature of the ions and is known to follow the Hofmeister series or lyotropic series.[12,14,33]

cations: $Mg^{2+} > Li^+ > Na^+ > K^+ > NH_4^+$ (A)

anions: $SO_4^{2-} > HPO_4^{2-} > CH_3COO^- > Cl^- > Br^- > NO_3^- > I^- > ClO_4^- > SCN^-$ (B)

Anions have a greater effect on water structure than do the cations and differences between monovalent cations are generally less significant than the differences between the monovalent anions. In order to identify the predominant effect responsible for the destabilization observed at high salt concentration on the PNA complexes, we have studied the effects of a series of Na^+ salts with different monovalent anions CH_3COO^-, Cl^-, and ClO_4^- on the stability of the PNA−PNA and N/3′ PNA−DNA duplexes.

The change in T_m vs Na-salt concentration (1−5 M) is shown for the PNA−PNA duplexes in Figure 5a and for N/3′ PNA−DNA in Figure 5b. In both cases the destabilizing effects observed with increasing salt concentration of the respective anions follow the Hofmeister series. The CH_3COO^- shows least destabilization followed by Cl^- with a maximum destabilization observed in the presence of ClO_4^-. The difference in the effect of CH_3COO^- and Cl^- in the N/3′ PNA−DNA duplex is less significant than that in the PNA−PNA duplex.

Structural Studies by Circular Dichroism. Conformational information was obtained by circular dichroism (CD) studies, at different temperatures and salt concentrations. The CD spectrum of the antiparallel N/3′ PNA−DNA is similar to that of the DNA B-helix suggesting a B-like conformation.[6] How-

(30) Olson, W. K.; Manning, G. S. *Biopolymers* **1976**, *15*, 2391−2405.
(31) Anderson, C. F.; Record, M. T., Jr. *Annu. Rev. Biophys. Biophys. Chem.* **1990**, *19*, 423−465.
(32) Sharp, K. A.; Honig, B. *Annu. Rev. Biophys. Biophys. Chem.* **1990**, *19*, 301−332.
(33) Hamaguchi, K.; Geiduschek, E. P. *J. Am. Chem. Soc.* **1962**, *84*, 1329−1338.
(34) Fenley M. O.; Manning G. S.; Olson W. M. *Biopolymers* **1990**, *30*, 1191−1203.
(35) Zieba, K.; Chu, T. M.; Kupke, D. W.; Marky, L. A. *Biochemistry* **1991**, *30*, 8018−8026.

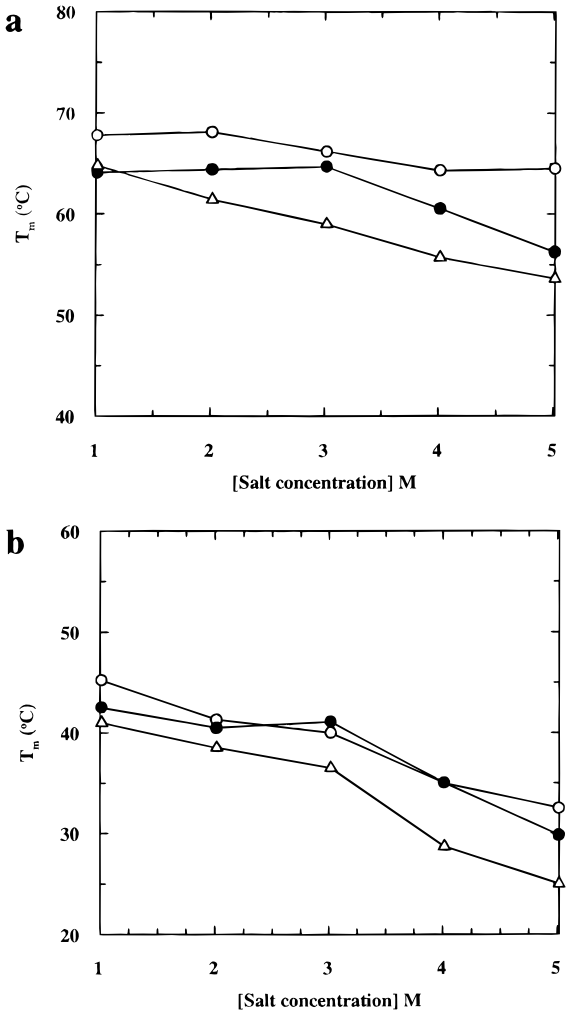

Figure 5. Effects of high (1−5 M) ionic strength on the thermal stability of (a) PNA−PNA and (b) N/3′ PNA−DNA in CH_3COONa (○), NaCl (●), or $NaClO_4$ (△).

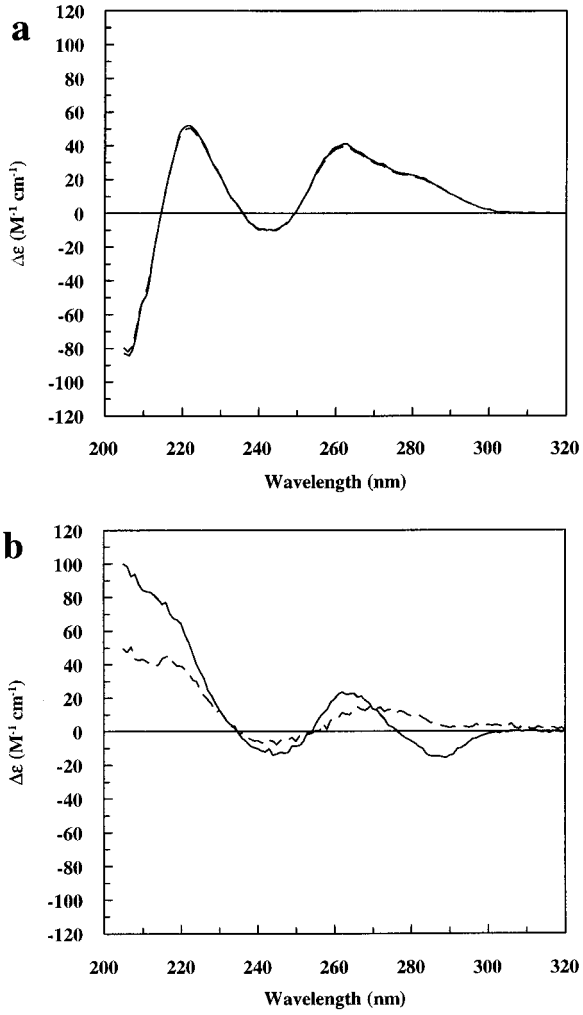

Figure 6. Circular dichroism spectra of (a) N/3′ PNA−DNA duplex at low ionic strength, 0 M NaCl (—), and high ionic strength, 500 mM NaCl (- - -), in 10 mM sodium phosphate buffer at pH 7.0. The strand concentration was 7 μM and the temperature 20 °C. (b) The N/5′ PNA−DNA duplex at low ionic strength, 0 M NaCl (—), and high ionic strength, 500 mM NaCl (- - -), in 10 mM sodium phosphate buffer at pH 7.0. The strand concentration was 5 μM.

ever, the CD spectrum for the N/5′ PNA−DNA duplex is significantly different from that of the N/3′ PNA−DNA duplex.

Figure 6a shows that addition of NaCl did not significantly affect the CD spectra of the N/3′ PNA−DNA duplexes. Similar results were obtained in the case of PNA−PNA (with a helicity inducing terminal lysine residue[7]) and DNA−DNA duplexes (data not shown). The CD spectrum of the N/5′ PNA−DNA duplex mixed in the presence of NaCl (500 mM NaCl) showed a substantial difference to that of the N/5′ duplex as seen in Figure 6b. However, when salt was added to the fully formed duplex, the CD spectrum did not show much dependence on salt concentration. We found that the CD spectrum of the parallel duplex at 500 mM NaCl could be reproduced by the weighted sum of the parallel DNA−PNA duplex in the absence of salt and a contribution from single-stranded DNA (the single stranded PNA, without a terminal lysine, gives no CD signal[7]). It is obvious that the difference in the CD spectra of parallel DNA−PNA duplex at low salt (0M NaCl) and high salt (500 mM) concentrations can be explained by the presence of single-stranded PNA and DNA at the high salt concentration.

It was found that the parallel duplex formation at room temperature was very slow, taking several hours for complete formation in buffer without added salt. It should be mentioned that similar slow formation of duplex was observed both for N/3′ and N/5′ PNA−DNA duplexes when the $MgCl_2$ concentration was increased from 0 to 50 mM. In contrast, the N/3′ DNA−PNA (both in 0 and 500 mM NaCl) duplex forms in <1 min after mixing the single-stranded components with or without salt at 20 °C.

Discussion

It is of interest to understand why the antiparallel duplexes involving PNA and PNA−PNA show higher stability at low ionic strength than the corresponding DNA−DNA duplexes (Figure 2). The response of these duplexes involving PNA to the change in the ionic environment is also distinctly different from that of a DNA−DNA duplex having the same base sequence as the PNA complexes (Table 1).

Salts are known to exert their effects on the stability of biopolymers mainly through electrostatic interactions at low to moderate salt concentrations (≤0.5 M) and predominantly through the indirect effect on bulk aqueous solvent at high salt concentrations (≥1 M), where the electrostatic contributions saturate. The effect of a monovalent salt such as NaCl on the thermal stability of the different duplexes has been investigated in some detail here (Figure 3a,b) as a prototype of the simplest case. We thereby avoided possible complications with specific binding of higher valence cations such as Mg^{2+} and spermine.

At low to moderate NaCl concentration (≤0.5 M) the polyelectrolyte character of N/3′ PNA−DNA predominates. This

is shown by the additional destabilization of the N/3′ PNA−DNA duplex compared to the uncharged PNA−PNA duplex, which shows little or no change in the T_m values in this concentration range (Figure 3a). This dependence of the T_m values on the ionic strength for the N/3′ PNA−DNA duplex is independent of the chain length and the presence of single positive charge on the PNA strand (Figure 3b). The T_m vs log-[Na^+] plots were used to estimate the number of thermodynamic counterions condensed or released per phosphate ($\Delta\psi$) based on the counterion condensation theory (Table 3 and Figure 4a) on duplex formation for the DNA−DNA and N/3′ PNA−DNA, respectively. The evaluated $\Delta\psi$ value of 0.15 for the 10-mer DNA−DNA duplex is close to that reported for polymeric DNA ($\Delta\psi = 0.17$).[19,21] This indicates that even short oligonucleotides of 10 base pairs electrostatically behave essentially as long rods.[34,35] The $\Delta\psi$ value of −0.05 for N/3′ PNA−DNA (10-mer) indicates a small but significant amount of counterion release upon duplex formation.

The T_m vs log[Na^+] dependence was analyzed further using the counterion condensation theory or the Poisson−Boltzmann model. The CC theory, approximating the molecules with linear arrays of charges, requires an increase in linear charge separation of ∼1 Å (as compared with canonical B-DNA, i.e. from 3.4 to 4.4 Å) for the N/3′ PNA−DNA duplex. With the PB model based on a cylindrical approximation of the helices, using the earlier estimated cylindrical dimensions of coil DNA, and assuming half the linear charge density of the N/3′ PNA−DNA duplex as compared to the DNA−DNA duplex, we find that a cylinder radius of 8.6 Å fits the melting data. In this model therefore the cylindrical dimensions of the PNA−DNA helix ($a_h = 8.6$ Å, $b_h = 3.4$ Å) are quite similar to the dimensions of the DNA−DNA helix ($a_h = 9.4$ Å, $b_h = 3.4/2$ Å), and fully consistent with a B-like structure of PNA−DNA helices.[6,8]

There is no support in the current literature for a ∼1-Å increase in helical rise for the PNA−DNA duplex as compared to the DNA−DNA duplex. The only helix involving PNA for which the crystal structure is known is a PNA·PNA−DNA triplex, which has a helical rise of 3.4 Å.[4] Our results show that the PB approach to evaluate the ionic effects on T_m for polyelectrolytes gives a more realistic description of our system. Similar conclusions have been drawn in earlier studies on DNA.[23,25,36]

Thermodynamic Profiles for Duplex Formation. The overall free energy (ΔG) is formally subdivided into an enthalpic (ΔH) and an entropic (ΔS) contribution. As can be seen (Table 2) the additional stability of the N/3′ PNA−DNA duplex (ΔG ∼ 7 kcal/mol more favorable) over a DNA−DNA duplex is due to the more favorable entropic contribution. The enthalpy changes ΔH for both duplexes are not very different. This indicates a B-like double-helical structure in both cases, consistent with the NMR results on the same 10-mer N/3′ PNA−DNA.[8] The similar hypochromicity values obtained for the two duplexes also reflect this fact. The entropic contribution to the enhanced stability of the N/3′ PNA−DNA duplex over the corresponding DNA−DNA duplex is ascribed directly to the ion release associated with the N/3′ PNA−DNA duplex formation.

In the case of the PNA−PNA duplex the higher stability compared to that of the DNA−DNA (ΔG 12 kcal/mol more favorable) is due to the enthalpic rather than the entropic contribution. Since the ΔH values represent the enthalpy differences between the coil state and the duplex state of the system, a larger value of ΔH implies that there is a larger structural rearrangement in going from one state to another in the PNA−PNA case as compared to the DNA−DNA case. The larger hypochromicity values for the PNA−PNA compared to the DNA−DNA duplex is consistent with this explanation.

Destabilization of the Duplexes in High Salt Concentration. At high salt concentration (NaCl > 1 M) where the electrostatic contributions saturate (Figure 3) the presence of backbone charges can no longer dominate the interactions. This is reflected in the decrease in the T_m for all three types of duplexes, which follow a similar trend irrespective of their backbone charges (Figure 3a,b). As mentioned earlier, neutral salts in high concentration (>1 M) exert their specific effect on the stability of the macromolecular structure like proteins either through their indirect effect on the aqueous solvent or through their preferential interactions with the macromolecule itself.[37] We have chosen three monovalent anions from the Hofmeister series, CH_3COO^-, Cl^-, and ClO_4^-, keeping Na^+ as the cation (Figure 5). It has been shown for a series of Na salts that the effects of these salts manifest themselves in the preferential increase in the surface free energy per unit area or the surface tension at the macromolecule−solvent interface, which follows the Hofmeister series.[38] Therefore the Hofmeister series for these anions correlates well with the preferential increase in the hydrophobic interactions between nonpolar molecules in their presence following the order $CH_3COO^- > Cl^- > ClO_4^-$. The fact that the destabilization effects of these anions at high salt concentration follow the Hofmeister series indicates that hydrophobic interactions play a dominant role in the stability of the PNA−PNA as well as the N/3′ PNA−DNA duplexes.

JA960495L

(36) Guéron, M.; Weisbuch, G. *Biopolymers* **1980,** *19*, 353−382.

(37) Arakawa, T.; Timasheff, S. N. *Biochemistry* **1984**, *23*, 5912−5923.

(38) Arakawa, T.; Timasheff, S. N. *Biochemistry* **1982**, *21*, 6545−6552.